

Reactor simulation uncertainties analysis for reactor antineutrino experiment using sampling method [☆]

X.B.Ma^a, J.Y.Liu^a, J.Y.Xu^a, F.Lu^a, Y.X.Chen^a

^a*North China Electric Power University, Beijing 102206, China*

Abstract

Antineutrino spectrum prediction is critical for reactor antineutrino experiment. Reactor simulation is an important uncertainty source for the antineutrino spectrum prediction. However, previous study did not shown what is the uncertainty source of reactor simulation. In this study, Monte Carlo-based sampling method was proposed to evaluated the fission fraction uncertainties. It was found that fission cross section uncertainties are important uncertainty source for ^{235}U , ^{239}Pu and ^{241}Pu , but for ^{238}U , elastic cross section and inelastic cross section is important. For the manufacturing parameters, the ^{235}U enrichment is the main uncertainty. The uncertainties induced by the burnup were evaluated through the uncertainty of atomic density of the four isotopes. The total fission fraction uncertainty in reactor simulation are 0.83%, 2.24%, 1.79% and 2.59% for ^{235}U , ^{238}U , ^{239}Pu and ^{241}Pu , respectively.

Keywords:

reactor neutrino experiment, uncertainties analysis, fission fraction, Sampling method

1. Introduction

Reactor antineutrinos are used in the study of neutrino oscillations and in the search for signatures of nonstandard neutrino interactions, as well as to monitor reactor conditions to safeguard operations. In the analysis, the antineutrino flux is an important source of uncertainties associated with measurements in reactor neutrino experiments. Usually, the following formula is

[☆]Corresponding author

Email address: maxb@ncepu.edu.cn (X.B.Ma)

used to calculate the antineutrino spectrum for one reactor,

$$S(E_\nu) = \frac{W_{th}}{\sum_j f_j e_j} \sum_i f_i S_i(E_\nu), \quad (1)$$

where W_{th} (MeV/s) is the reactor thermal power, f_j the fission fraction associated with each isotope (^{235}U , ^{238}U , ^{239}Pu and ^{241}Pu), e_j the thermal energy release per fission for each isotope, $S_i(E_\nu)$ a function of the $\bar{\nu}_e$ energy E_ν signifying the $\bar{\nu}_e$ yield per fission for each isotope. In order to evaluate the uncertainties in the reactor simulation, the calculated concentration of each isotopes using different reactor simulation code were compared with the benchmark[1], and a proximate method was proposed to determine the fission fraction uncertainty by using concentration uncertainty. Using the Takahama-3 benchmark and the largest burnup sample were calculated with MURE and DRAGON, the concentration differences of each isotopes between calculated value and experiment data are about 5%[2]. The fission fraction of Daya bay reactor were also simulated using DRAGON and comparison was performed with that obtained with SCIENCE code which was used in the Daya bay nuclear power plant. It was found the average deviation for ^{235}U , ^{238}U , ^{239}Pu and ^{241}Pu are 0.71%, 4.2%, 2.1% and 3.5%[3], respectively. On the other hand, the fission fraction uncertainty as a function of burnup did not given. In order to investigate this question and to determine the correlation coefficient of fission fraction of different isotopes, a new Monte Carlo-based method were proposed using the one group fission cross section and concentration of each isotopes and the correlation coefficient with the function of burnup was also discussed[4]. However, previous studies did not solve the question what is the main uncertainty source of fission fraction, the purpose of this study was to investigate fission fraction uncertainties induced by neutron cross section data and other fuel manufacturing uncertainties which are used in the reactor simulation.

This paper is structured as follows. Monte Carlo-based sampling method using for evaluation of uncertainties of fission fraction was introduced in Section 2. In order to generate library sample for the transport calculation, SUACL (Sensitivity and Uncertainty Analysis Code for Light water reactor) were developed, and TMI-1 benchmark and one MOX test were used to perform the verification in Section 3. All the reaction type of the four isotopes and other important isotopes, atomic density uncertainties induced by burnup, and manufacturing parameters are taken into account to evaluate uncertainty of fission fraction in Section 4. The last section is the conclusion.

2. Monte Carlo-Based sampling method

In the reactor simulation, we always focus on the neutronics characteristics because that fission power and neutron chain fission reaction are determined by the neutron flux, and therefore, reactor simulation is also called as neutronics calculation. Various uncertainties affect the simulation results. In the case of reactor simulation, material composition, geometry, operation conditions, measurement plant data, neutron cross section, approximation in the simulation models, etc., would have an impact on calculation results. In the present study, the impact of cross section uncertainty and fuel manufacturing parameters on the fission fraction results are discussed.

Propagation of cross section uncertainties to core characteristics has been traditionally evaluated by the sandwich formula[5, 6]. There are three difficulties by using sandwich formula for Pressure Water Reactor (PWR) uncertainty analysis, such as complicated calculation sequence in typical PWR analysis, nonlinear effects of thermal hydraulics and burnup on the calculation results and the number of input and output parameters is large. Recently, the Monte Carlo-based sampling method has attracted attention since it can avoid the major difficulties shown in the above. The procedures for uncertainty estimation of fission fraction for antineutrino experiment using Monte Carlo based sampling method is shown Fig.1.

Generally, all cross section can be divided into the basic and integral ones. The integral cross sections are composed of basic cross sections. The cross section uncertainties are stored in their covariance data. Different evaluate approaches used in nuclear data library may lead to the different of analysis result. The covariance data which was used in present study were made using NJOY code[7] based on ENDF/B-VII.1[8] and JENDL4.0[9]. The covariance matrix of ^{235}U and ^{238}U for (n,γ) cross section are show in Fig.2. Other important inputs are the parameters of fuel/assembly manufacturing classified as the engineering parameters[12], which are crucial to the simulation model. The uncertainty of these parameters can propagate to the result through the simulating model and affect the accuracy of the result. The code SUACL based on Monte Carlo sampling method were programmed to do the uncertainty analysis of neutron cross section and manufacturing parameters.

In the Monte Carlo based sampling method, a sample is randomly taken from the parent population. In the present study, multi-group microscopic cross sections are randomly sampled using the covariance matrix. Sets of sampled cross sections approximately represent the distribution of the micro-

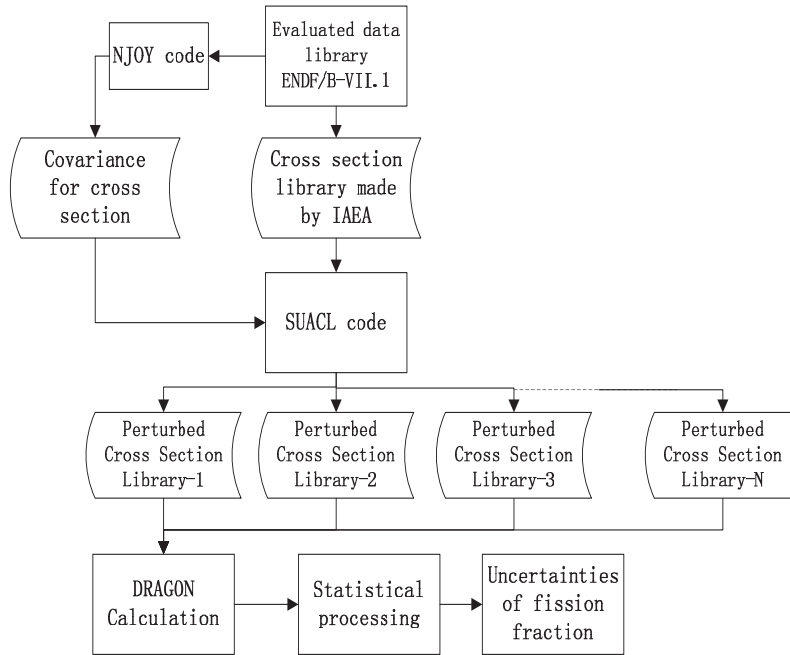


Fig. 1: The procedures for uncertainty estimation of fission fraction for antineutrino experiment using Monte Carlo based sampling method

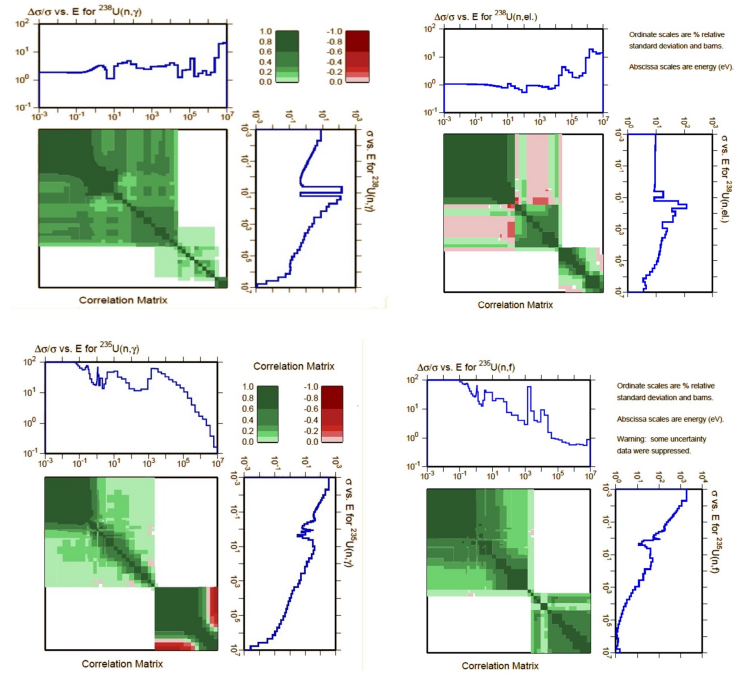


Fig. 2: The covariance matrix of ^{235}U and ^{238}U for (n, γ) cross section

scopic due to a natural characteristics of measurement error. Cross sections are randomly perturbed[13] by

$$\sigma_{x,g}^{per} = P_{x,g} \times \sigma_{x,g} \quad (2)$$

where $P_{x,g}$ perturbation factor for microscopic cross section, $\sigma_{x,g}^{per}$ perturbed microscopic cross section, $\sigma_{x,g}$ unperturbed microscopic cross section in the original cross section library, x type of cross section, and g energy group. Multigroup, microscopic cross sections in the original cross section library are perturbed by Eq.(2) to generate the perturbed cross section library. A procedure for generating vectors of dependent random variables consistent with a given covariance matrix involves performing a spectral decomposition of the matrix.

$$\Sigma = \mathbf{V} \times \mathbf{D} \times \mathbf{V}^T. \quad (3)$$

The matrix of relative covariance, Σ , is decomposed into three matrices, where \mathbf{V} is a matrix whose columns are eigenvectors of Σ , and \mathbf{D} is a diagonal matrix of eigenvalues that correspond to the eigenvectors in \mathbf{V} . $\Sigma^{1/2}$ matrix is defined as

$$\Sigma^{1/2} = \mathbf{V} \times \mathbf{D}^{1/2} \times \mathbf{V}^T \quad (4)$$

where $D^{1/2}$ is a diagonal matrix whose elements are the roots of the elements in \mathbf{D} . The perturbed factor can be calculated using the Eq.5[14].

$$\mathbf{P}(\Sigma) = \Sigma^{1/2} \mathbf{G}(0, 1) + \mathbf{I} \quad (5)$$

where \mathbf{G} is a vector of n normally distributed dependent random variables with a mean of zero and standard deviation of one, and \mathbf{I} is unitary matrix.

3. Validation of SUACL for PWR pin cell analysis

In order to perform the fission fraction uncertainty in the reactor simulation using Monte Carlo sampling method, SUACL[10] were developed. The perturbed nuclear library is generated by SUACL as shown in Fig.1, and reactor simulation code DRAGON[11] applying the perturbed nuclear library to do the transport calculation. To do the verification of SUACL code, TMI-1 PWR fuel cell benchmark [12] and MOX cell was used. Parameters of TMI-1 and MOX are shown in Table 1. The uncertainty of infinity multiplication factor of TMI-1 and MOX cell which were evaluated using SUACL are shown in Table 2. It can be found that results of SUACL are consistent with

Table 1: Parameters of TMI-1 and MOX cell

Parameters	MOX cell	TMI-1 cell
Fuel material	(U,Pu)O ₂	UO ₂
Gap material	N/A	He gas
Cald material	Zircaloy-4	Zircaloy-4
Moderator	H ₂ O	H ₂ O
Fuel pellet/mm	9.020	9.391
Gap thickness/mm	0.0	0.955
Clad thickness/mm	0.380	0.673
Unit cell pith/mm	12.60	14.427

that of other code for the TMI-1 cell, and for the MOX cell, uncertainty of k_{inf} calculated by SUACL for each reaction channel are good well with that of TSUNAMI-1D. In this study, the covariance matrix was generated using NJOY based on ENDF/B-VII.1[8]. It can be seen that the code SUACL and the covariance matrix have been developed correctly and which can be used for the fission fraction uncertainty evaluation for the reactor antineutrino experiment.

4. Reactor simulation uncertainty for antineutrino experiment

There are four isotopes, such as ²³⁵U, ²³⁸U, ²³⁹Pu and ²⁴¹Pu, which are important to antineutrino experiment because of more than 99.0% emitting from these isotopes. To predict antineutrino flux for antineutrino experiment, fission fraction of each isotopes are needed according to Eq.(1). The process of evaluating fission fraction are depended with reactor simulation about the discipline of neutron. In general, the neutron behavior is described neutron transport equation and the cross sections of neutron with matter are the coefficient of the transport equation. Fission fraction of isotopes f_i ($i=^{235}\text{U}$, ²³⁸U, ²³⁹Pu and ²⁴¹Pu) can be defined as

$$f_i = \frac{N_i \sum_{g=1}^G \sigma_{i,g,f} \phi_g}{\sum_i N_i \sum_{g=1}^G \sigma_{i,g,f} \phi_g} \quad (6)$$

where $\sigma_{i,g,f}$ is the microscopic cross section of isotopes i in g group, g the neutron energy number, G the total neutron energy group number, N_i the atomic density of isotopes, ϕ_g the neutron flux of group g which would be

Table 2: Uncertainty of infinity multiplication factor k_{inf} (%)

Isotopes	Reaction Parameters	CASMO-4[15]	TSUNAMI[16]	UNICORN[17]	SUACL
UO ₂					
²³⁸ U	$\sigma_{n,\gamma}$	0.325	0.284	0.377	3.94
²³⁸ U	$\sigma_{elastic}$	0.039	0.106	0.114	0.211
²³⁵ U	$\sigma_{n,\gamma}$	0.223	0.210	0.196	0.209
²³⁵ U	σ_f	0.078	0.077	0.079	0.084
H	σ_s	0.027	0.026	0.038	0.037
MOX					
²³⁹ Pu	$\sigma_{n,\gamma}$	N/A	0.204	N/A	0.211
²³⁹ Pu	σ_f	N/A	0.192	N/A	0.182
²⁴⁰ Pu	$\sigma_{n,\gamma}$	N/A	0.088	N/A	0.063
²⁴² Pu	$\sigma_{n,\gamma}$	N/A	0.012	N/A	0.011
²³⁸ U	$\sigma_{n,\gamma}$	N/A	0.215	N/A	0.284
²³⁸ U	σ_f	N/A	0.018	N/A	0.017
²³⁵ U	$\sigma_{n,\gamma}$	N/A	0.061	N/A	0.059
²³⁵ U	σ_f	N/A	0.025	N/A	0.020
H	$\sigma_{elastic}$	N/A	0.038	N/A	0.030

$\sigma_{n,\gamma}$ represent capture cross section, σ_f fission cross section, $\sigma_{elastic}$ elastic scattering cross section

calculated by DRAGON. From Eq.6, we can see that the uncertainties of fission fraction can be divide into three parts. First parts is atomic density uncertainty caused by burnup, second parts is fission cross section uncertainty and third parts is neutron flux uncertainty caused by other cross sections and parameters.

The Daya Bay reactor operates with 157 fuel assemblies producing a total thermal power of 2895MW. The assembly is a 17×17 design, for a total of 289 rods. There are 264 fuel rods, 24 control rods, and one guide tube. The enrichment of the new fuel of the Daya Bay reactor core is 4.45% for the 18-month reloaded core design[18]. About 1/3 fuel in the core will be reloaded. The atomic density of four isotopes as a function of burnup is shown in Fig.3, and the fission fraction as a function of burnup is shown in Fig.4. The fission fraction of ^{235}U decrease with the burnup increasing mainly because of atomic density decreasing. However, ^{239}Pu has opposite trend mainly because of atomic density increasing.

The cross section are one of main uncertainties source of fission fraction evaluation. The most important reaction types of each isotopes, such as fission cross section σ_f , capture cross section $\sigma_{n,\gamma}$, elastic cross section σ_{elas} , inelastic cross section σ_{inelas} and neutron number per fission ν , have been taken into account. The fission fraction uncertainties of each isotopes caused by different reaction type of each isotopes at Begin Of Cycle (BOC), Middle Of Cycle (MOC) and End Of Cycle (EOC) have been shown in table 3, table 4 and table 5, respectively. When we evaluated the fission fraction uncertainties at the MOC and EOC, the uncertainties of cross section were taken into account, and neglect the uncertainties of atomic density. The uncertainties of atomic density because of burnup calculation would be taken into account in the following. From table 3, table 4 and table 5, two major conclusion can be drawn from those results. First, fission cross section are the main contribution to the uncertainties of fission fraction because that its uncertainties directly propagate to fission fraction, and other cross section uncertainties is indirectly propagation to fission fraction through neutron flux uncertainties. Second, fission fraction uncertainties of ^{235}U , ^{239}Pu and ^{241}Pu are induced by the thermal incident neutron because that they are fissile and have large fission cross section in the low energy. however, for ^{238}U , its uncertainty is induced by the fast neutron because that it is fissionable and only when the incident neutron energy is larger than fission threshold energy. The relative error of fission cross section are shown in Fig.5. Although the relative error of ^{238}U in the low energy is very large, the relative error in the

high energy is relative small. Therefor, fission fraction uncertainty of ^{238}U is not so large. fission fraction uncertainty of ^{238}U is dominated by the elastic and inelastic cross section as shown in Fig.4 because of large relative error in the high energy region for elastic and in elastic cross section.

Atomic density of four isotopes would be varied because of transmutation and fission during reactor operation. Atomic density uncertainties come from the uncertainties of decay data, fission yields and neutron flux. Results obtained in table 3, table 4 and table 5 neglecting number density uncertainties. Atomic density uncertainties as a function of burnup when propagating incident neutron data uncertainties according to ENDF/B-VII.1 covariance data was studied[20]. Atomic density uncertainties are taken place at the end of cycle (60GW.d/tU), and the largest uncertainties of ^{235}U , ^{239}Pu and ^{241}Pu are 2.15%, 2.0%, 1.91%, respectively. The uncertainty of ^{238}U is less than 1.0%. In order to evaluate fission fraction uncertainties conservatively which induced by atomic density, the uncertainty of ^{238}U is assumed as 1.0%. Fission fraction uncertainties induced by atomic density as a function of burn-up are shown in table 6, and which are 0.831%, 0.233%, 1.83% and 2.26% for ^{235}U , ^{238}U , ^{239}Pu and ^{241}Pu , respectively.

Fuel or assembly manufacturing uncertainties, such as enrichment, pellet density, cladding dimensions, burnable poison (BP) concentration, and assembly geometry, are also the uncertainties source of reactor simulation. The following manufacturing uncertainties in terms of 3σ are provided in ref[12]. Fission fraction uncertainties caused by manufacturing parameters in terms of 1σ have been shown in table 7. It can be found that the ^{235}U enrichment uncertainties are the main uncertainties in all the manufacturing parameters, and other manufacturing parameter uncertainty are small.

Considering all the effects which have been given above, the total uncertainties of fission fraction in reactor simulation is shown in table 8. It can be seen that The total fission fraction uncertainty in reactor simulation are 0.90%, 2.09%, 1.92% and 2.69% for ^{235}U , ^{238}U , ^{239}Pu and ^{241}Pu , respectively.

5. Conclusion

Reactor simulation uncertainties are evaluated by using atomic density comparison calculation with experiment in previous study. In this study, Monte Carlo-based sampling method was proposed to evaluated the fission fraction uncertainties. It was found that fission cross section uncertainties are important uncertainty source for ^{235}U , ^{239}Pu and ^{241}Pu , but for ^{238}U , elastic

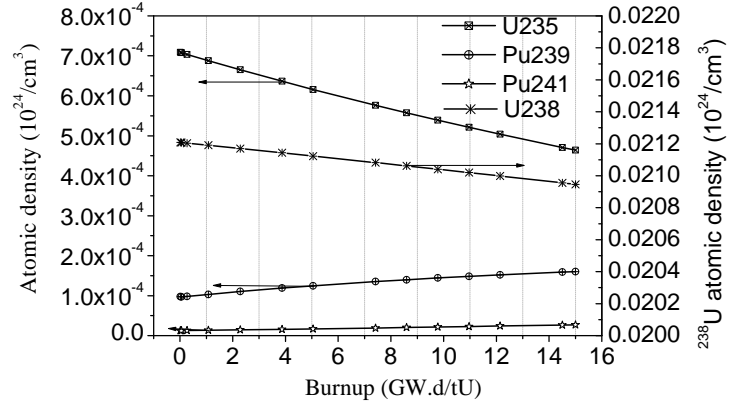


Fig. 3: Atomic density as a function of burnup

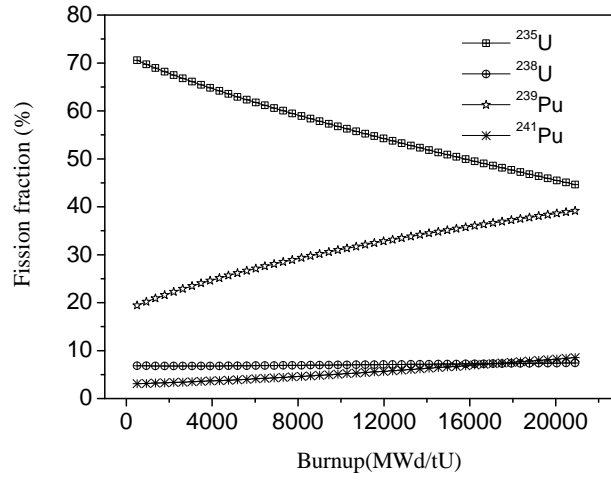


Fig. 4: Fission fraction of ^{235}U , ^{238}U , ^{239}Pu and ^{241}Pu as a function of burnup calculated by DRAGON

Table 3: Relative fission fraction uncertainties induced by different reaction type at the Begin Of Cycle (BOC)(%)

Isotopes	Reaction Channel	^{239}Pu	^{241}Pu	^{235}U	^{238}U
^{235}U	σ_f	2.37E-1	2.47E-1	1.22E-1	6.59E-2
	$\sigma_{n,\gamma}$	7.68E-3	4.68E-3	7.66E-3	7.16E-2
	σ_{inelas}	3.69E-4	3.79E-4	3.66E-4	5.23E-3
	σ_{elas}	5.74E-4	5.83E-4	5.65E-4	8.06E-3
	ν	1.66E-2	1.46E-02	1.07E-2	1.81E-1
^{238}U	σ_f	3.14E-2	3.13E-2	3.11E-2	4.62E-1
	$\sigma_{n,\gamma}$	1.44E-2	2.15E-2	1.51E-2	2.10E-1
	σ_{inelas}	6.79E-2	7.02E-2	6.79E-2	9.94E-1
	σ_{elas}	9.65E-2	1.00E-1	9.54E-2	1.42E-0
	ν	2.83E-3	2.49E-3	1.82E-3	3.09E-2
^{239}Pu	σ_f	5.91E-1	2.42E-1	2.32E-1	4.26E-2
	$\sigma_{n,\gamma}$	3.04E-2	9.44E-3	8.52E-3	6.41E-2
	σ_{inelas}	1.02E-4	1.05E-4	1.02E-4	1.44E-3
	σ_{elas}	1.70E-4	1.74E-4	1.68E-4	2.40E-3
	ν	1.75E-3	1.54E-3	1.13E-3	1.91E-3
^{241}Pu	σ_f	4.91E-2	1.42E0	4.84E-2	9.73E-3
	$\sigma_{n,\gamma}$	1.12E-3	1.38E-3	4.68E-4	9.82E-3
	σ_{inelas}	2.87E-5	2.85E-5	2.84E-5	3.88E-4
	σ_{elas}	1.74E-5	2.28E-5	1.78E-5	2.17E-4
	ν	7.77E-4	6.86E-4	5.01E-4	8.50E-3
^{16}O	σ_{inelas}	5.45E-5	5.41E-5	5.48E-5	7.83E-4
	σ_{elas}	7.15E-2	3.46E-2	1.62E-2	4.42E-1
H	σ_{elas}	5.45E-2	6.72E-2	6.18E-2	8.92E-1
Total		6.58E-01	1.47E+00	3.00E-1	2.08E+0

$\sigma_{n,\gamma}$ represent capture cross section, σ_f fission cross section, σ_{elas} elastic scattering cross section, σ_{inelas} inelastic scattering cross section, ν neutron number per fission

Table 4: Relative fission fraction uncertainties caused by different reaction type at the Middle Of Cycle (MOC)(%)

Isotopes	Reaction Channel	²³⁹ Pu	²⁴¹ Pu	²³⁵ U	²³⁸ U
²³⁵ U	σ_f	2.14E-1	2.22E-1	1.45E-1	6.06E-2
	$\sigma_{n,\gamma}$	5.21E-3	4.22E-3	7.47E-3	5.87E-2
	σ_{inelas}	3.70E-4	3.84E-4	3.70E-4	5.36E-3
	σ_{elas}	5.76E-4	5.90E-4	5.73E-4	8.28E-3
	ν	1.32E-2	1.16E-2	8.48E-3	1.49E-1
²³⁸ U	σ_f	3.20E-2	3.19E-2	3.17E-2	4.61E-1
	$\sigma_{n,\gamma}$	1.41E-2	2.17E-2	1.61E-2	2.12E-1
	σ_{inelas}	6.91E-2	7.15E-2	6.84E-2	9.94E-1
	σ_{elas}	9.82E-2	1.02E-1	9.71E-2	1.42E-0
	ν	2.72E-3	2.40E-3	1.75E-3	3.07E-2
²³⁹ Pu	σ_f	5.41E-1	2.85E-1	2.71E-1	5.13E-2
	$\sigma_{n,\gamma}$	3.57E-2	9.13E-3	1.39E-2	7.61E-2
	σ_{inelas}	1.35E-4	1.41E-4	1.35E-4	1.96E-3
	σ_{elas}	2.23E-4	2.35E-4	2.67E-4	3.28E-3
	ν	2.30E-3	2.03E-3	1.48E-3	2.60E-2
²⁴¹ Pu	σ_f	7.58E-2	1.40E0	7.51E-2	1.65E-2
	$\sigma_{n,\gamma}$	1.60E-3	1.92E-3	4.58E-4	1.33E-2
	σ_{inelas}	4.13E-5	4.17E-5	4.10E-5	5.79E-4
	σ_{elas}	2.63E-5	3.38E-5	2.30E-5	3.12E-4
	ν	1.14E-3	1.01E-3	7.36E-4	1.29E-2
¹⁶ O	σ_{inelas}	5.49E-5	5.80E-5	5.97E-5	8.22E-4
	σ_{elas}	6.94E-2	2.95E-2	9.74E-3	4.36E-1
H	σ_{elas}	5.85E-2	6.95E-2	6.27E-2	8.95E-1
Total		6.08E-1	1.45E+0	3.46E-1	2.07E+0

$\sigma_{n,\gamma}$ represent capture cross section, σ_f fission cross section, σ_{elas} elastic scattering cross section, σ_{inelas} inelastic scattering cross section, ν neutron number per fission

Table 5: Relative fission fraction uncertainties caused by different reaction type at the End Of Cycle (EOC)(%)

Isotopes	Reaction Channel	²³⁹ Pu	²⁴¹ Pu	²³⁵ U	²³⁸ U
²³⁵ U	σ_f	1.81E-1	1.87E-1	1.80E-1	5.33E-2
	$\sigma_{n,\gamma}$	3.60E-3	3.87E-3	6.97E-3	4.81E-3
	σ_{inelas}	3.02E-4	3.14E-4	3.01E-4	4.34E-4
	σ_{elas}	4.69E-4	4.84E-4	4.71E-4	6.70E-3
	ν	1.06E-2	9.31E-03	6.84E-3	1.22E-1
²³⁸ U	σ_f	3.24E-2	3.23E-2	3.21E-2	4.61E-1
	$\sigma_{n,\gamma}$	1.37E-2	2.19E-2	1.70E-2	2.13E-1
	σ_{inelas}	6.70E-2	7.24E-2	6.93E-2	9.93E-1
	σ_{elas}	9.94E-2	1.03E-1	9.84E-2	1.42E-0
	ν	2.64E-3	2.33E-3	1.71E-3	3.05E-2
²³⁹ Pu	σ_f	4.83E-1	3.43E-1	2.29E-1	6.74E-2
	$\sigma_{n,\gamma}$	3.53E-2	7.93E-3	1.95E-3	8.98E-2
	σ_{inelas}	1.62E-4	1.68E-4	1.62E-4	2.34E-3
	σ_{elas}	2.73E-4	2.86E-4	2.74E-4	3.92E-3
	ν	2.67E-3	2.35E-3	1.73E-3	3.09E-3
²⁴¹ Pu	σ_f	1.11E-1	1.362	1.11E-1	2.59E-2
	$\sigma_{n,\gamma}$	1.99E-3	2.56E-3	6.49E-4	1.91E-2
	σ_{inelas}	5.82E-5	5.87E-5	5.89E-5	8.33E-4
	σ_{elas}	3.32E-5	4.42E-5	3.16E-5	4.52E-4
	ν	1.61E-3	1.42E-3	1.04E-3	1.86E-2
¹⁶ O	σ_{inelas}	5.78E-5	5.94E-5	6.39E-5	8.49E-4
	σ_{elas}	6.64E-2	2.51E-2	6.56E-3	4.31E-1
H	σ_{elas}	6.09E-2	7.08E-2	5.33E-2	8.99E-1
Total		5.51E-1	1.42E+0	4.15E-1	2.07E+0

$\sigma_{n,\gamma}$ represent capture cross section, σ_f fission cross section, σ_{elas} elastic scattering cross section, σ_{inelas} inelastic scattering cross section, ν neutron number per fission

Table 6: Fission fraction uncertainties caused by atomic density change during burnup (%)

Isotopes	²³⁹ Pu	²⁴¹ Pu	²³⁵ U	²³⁸ U
²³⁵ U (1.78%)	1.07E+00	1.12E+00	5.36E-01	1.93E-01
²³⁸ U (1.00%)	5.34E-02	6.03E-02	5.97E-02	8.24E-01
²³⁹ Pu (2.00%)	1.29E+00	5.56E-01	5.16E-01	7.24E-03
²⁴¹ Pu (1.91%)	7.17E-02	1.73E+00	7.10E-02	3.27E-03
Total	1.68E+00	2.14E+00	7.50E-01	8.46E-01

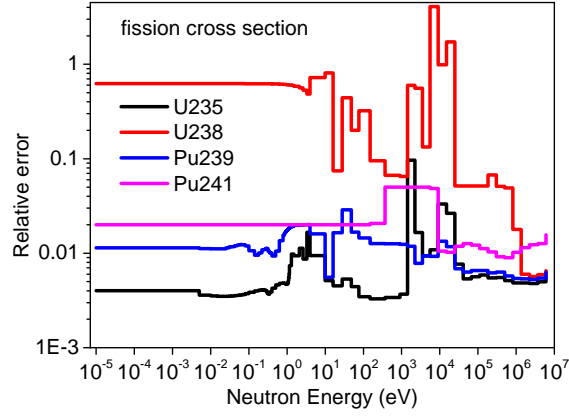


Fig. 5: fission cross section relative error vs the neutron energy

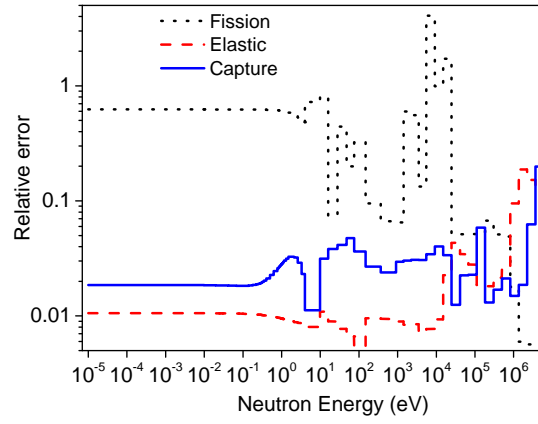


Fig. 6: Cross section relative error of ^{238}U vs the neutron energy

Table 7: Fission fraction uncertainties caused by manufacturing parameters (%)

Isotopes	Clad thickness	Pellet diameter	Fuel density	Gap thickness	^{235}U enrichment	Total
^{235}U	2.12E-15	5.37E-5	2.82E-4	5.45E-5	9.03E-3	9.04E-3
^{238}U	1.01E-15	6.99E-4	3.91E-3	7.21E-4	3.81E-3	5.55E-3
^{239}Pu	1.46E-15	2.80E-5	2.01E-4	3.04E-5	1.79E-2	1.79E-2
^{241}Pu	1.13E-15	5.6E-5	2.98E-4	6.10E-5	1.87E-2	1.87E-2

Table 8: Total fission fraction uncertainties(%)

Operation state	^{239}Pu	^{241}Pu	^{235}U	^{238}U
BOC	1.80	2.59	0.81	2.24
MOC	1.79	2.58	0.83	2.24
EOC	1.77	2.57	0.86	2.24

cross section and inelastic cross section is important. For the manufacturing parameters, the ^{235}U enrichment is the main uncertainty. The uncertainties induced by the burnup were evaluated through the uncertainty of atomic density of the four isotopes. The total fission fraction uncertainty in reactor simulation are 0.83%, 2.24%, 1.79% and 2.59% for ^{235}U , ^{238}U , ^{239}Pu and ^{241}Pu at the MOC, respectively.

Acknowledgments

The work was supported by National Natural Science Foundation of China (Grant No. 11390383) and the Fundamental Research Funds for the Central Universities(Grant No. 2015ZZD12), we would like to thank .

References

- [1] Z Djurcic, J A Detwiler, A Piepke, et al. Uncertainties in the anti-neutrino production at nuclear reactors, J.Phys.G: Nucl.Part.Phys. 2009, **36** : 045002
- [2] C. L. Jones, A. Bernstein,et.al. Reactor simulation for antineutrino experiments using DRAGON and MURE, Phys. Rev. D,2012,**86**:012001?

- [3] X.B. Ma, F. Lu, L.Z. Wang, et al. Uncertainty analysis of fission fraction for reactor antineutrino experiments, *Modern Physics Letters A*, 2016, Vol. 31, No. 20 : 1650120
- [4] X.B. Ma, R.M. Qiu, Y.X. Chen, et al. New Monte Carlo-based method to evaluate fission fraction uncertainties for the reactor antineutrino experiment, *Nuclear Physics A* 2017, **958**:211C218
- [5] D. G. CACUCI, *Sensitivity and Uncertainty Analysis: Theory*, Vol. 1, Chapman and Hall/CRC, Boca Raton, Florida, 2003.
- [6] Yousry Azmy, Enrico Sartori, *Nuclear computational science A Century in Review*, ISBN 978-90-481-3410-6, 2010, p219
- [7] R.E. MACFARLANE, A.C. KAHLER, "Methods for Processing ENDF/B-VII with NJOY", *Nuclear Data Sheets*, 111, 12, 2739 (2010) (see <http://t2.lanl.gov/codes/njoy99/>).
- [8] <http://www.nndc.bnl.gov/ndf/b7.1/>
- [9] <http://www.ndc.jaea.go.jp/jendl/j40/j40.html>
- [10] Jia Yi-Xu, Xu Bo-Ma, Fan Lu, et al. Nuclear Data and Fuel/Assembly Manufacturing Uncertainties Analysis and Preliminary Validation of SUACL, 2017 <https://arxiv.org/abs/1704.06601>
- [11] R.R.G. Marleau, A. Hebert and R. Roy, *A User Guide for DRAGON*, Technical Report, IGE-236 Rev. 1 (2001).
- [12] K. Ivanov, M. Avramova, S. Kamerow, et al. Benchmarks for uncertainty analysis in modelling (UAM) for the design, operation and safety analysis of LWRs, Volume I: Specification and Support Data for Neutronics Cases (Phase I), NEA/NSC/DOC(2013)7
- [13] Akio Yamamoto, Kuniharu Kinoshita, Tomoaki Watanabe, et al. Uncertainty Quantification of LWR Core Characteristics Using Random Sampling Method, *NUCLEAR SCIENCE AND ENGINEERING*, 2015, **181**: 1–15
- [14] MATTHEW RYAN BALL, *UNCERTAINTY IN LATTICE REACTOR PHYSICS CALCULATIONS*, McMaster University, 2011

- [15] Pusa M. Incorporation sensitivity and uncertainty analysis to a lattice physics code with application to CASMO-4, *Annals of Nuclear Energy*,2012, 40:153-162
- [16] B. T. Rearden, D. E. Mueller, S. M. Bowman, R. D. Busch, and S. J. Emerson, TSUNAMI Primer: A Primer for Sensitivity/Uncertainty Calculations with SCALE, ORNL/TM-2009/027, Oak Ridge National Laboratory, Oak Ridge, Tenn., January 2009
- [17] Wan Cheng-hui,Cao Liang-zhi,Wu Hong-chuan,et al. Eigenvalue Uncertainty Analysis Based on Statistical Sampling Method, *Atomic Energy Science and Technology*, 2015,49,11
- [18] Guangdong Nuclear Power Training Center, *Devices & Systems of 900 MW PWR*, Atomic Energy Press, ISBN7-5022-3171-4, 2005, pp.50–51.
- [19] Alain,Hebert, *Applied Reactor Physics*, press internationales polytechnique,2009,p6779
- [20] C.J.Diez,O.Buss,A.Hoefer, et al. Comparison of nuclear data uncertainty propagation methodologies for PWR burn-up simulations. *Annals of Nuclear Energy* 77 (2015) 101C114, arXiv:1411.0834v1,2014.